

High-rate intercity quantum key distribution with a semiconductor single-photon source

Jingzhong Yang,¹ Zenghui Jiang,¹ Frederik Benthin,¹ Joscha Hanel,¹ Tom Fandrich,¹ Raphael Joos,² Stephanie Bauer,² Sascha Kolatschek,² Ali Hreibi,³ Eddy Patrick Rugeramigabo,¹ Michael Jetter,² Simone Luca Portalupi,² Michael Zopf,¹ Peter Michler,² Stefan Kück,³ and Fei Ding^{1,4,*}

¹*Institut für Festkörperphysik, Leibniz Universität Hannover, Appelstraße 2, 30167 Hannover, Germany*

²*Institut für Halbleiteroptik und Funktionelle Grenzflächen,
Center for Integrated Quantum Science and Technology (IQST) and SCoPE,
University of Stuttgart, Allmandring 3, 70569 Stuttgart, Germany*

³*Physikalisch-Technische Bundesanstalt, Bundesallee 100, 38116 Braunschweig, Germany*

⁴*Laboratorium für Nano- und Quantenengineering, Leibniz Universität Hannover, Schneiderberg 39, 30167 Hannover, Germany*

Quantum key distribution (QKD) enables the transmission of information that is secure against general attacks by eavesdroppers. The use of on-demand quantum light sources in QKD protocols is expected to help improve security and maximum tolerable loss. Semiconductor quantum dots (QDs) are a promising building block for quantum communication applications because of the deterministic emission of single photons with high brightness and low multiphoton contribution. Here we report on the first intercity QKD experiment using a bright deterministic single photon source. A BB84 protocol based on polarisation encoding is realised using the high-rate single photons in the telecommunication C-band emitted from a semiconductor QD embedded in a circular Bragg grating structure. Utilising the 79 km long link with 25.49 dB loss (equivalent to 130 km for the direct-connected optical fibre) between the German cities of Hannover and Braunschweig, a record-high secret key bits per pulse of 4.8×10^{-5} with an average quantum bit error ratio of $\sim 0.65\%$ are demonstrated. An asymptotic maximum tolerable loss of 28.11 dB is found, corresponding to a length of 144 km of standard telecommunication fibre. Deterministic semiconductor sources therefore compete with state-of-the-art decoy state QKD with weak coherent pulses with respect to high secret key rate and have the potential to excel in measurement device independent protocols and quantum repeater applications.

I. INTRODUCTION

Realms of communication that transcend the limitations of traditional networks can be accessed by establishing a ‘quantum internet’ [1, 2] through the distribution of quantum light states. Sharing quantum bits of information with distant nodes via optical fibre or free space (satellite) enables new applications such as quantum teleportation [3–5], quantum cloud computing [6, 7] or quantum sensor networks [8, 9]. A primary advantage of quantum communication lies in its ability to ensure unambiguous security for modern communication networks, a security that is increasingly threatened by the rapid advancement of quantum computing technologies [10–12]. Hence, Quantum Key Distribution (QKD) has attracted worldwide attention for its unique ability to provide security based on the principles of quantum mechanics [13], surpassing the capabilities of classical cryptography [14].

The QKD landscape has evolved significantly over the years, using a variety of protocols and spanning fibre networks [15, 16] and satellite-to-ground free-space links [17, 18]. Despite this progress, the establishment of large networks currently requires the use of intermediate ‘trusted nodes’ [19], which provide limited security that can only be fully restored by the implementation of quantum repeaters [20]. Furthermore, conventional quantum light sources based on weak laser pulses [21] or spontaneous parametric down-conversion [22] struggle with a delicate balance between brightness and multiphoton emissions to resist photon number splitting attacks.

Decoy state QKD offers a potential solution [23], but at the cost of increased complexity and a penalty in the secret key rate (SKR) [19].

Semiconductor single photon sources (SPSs) hold immense potential in revolutionising large-scale quantum communication. Semiconductor quantum dots (QDs) are capable of emitting indistinguishable single photons on demand with unprecedented efficiency and purity [24, 25], offering strong advantages for QKD [26], including measurement device independent (MDI) schemes [27]. QDs also offer great prospects for the realisation of quantum repeaters, as they allow for inherent storage of quantum information [28] and can emit photonic cluster states [29]. The success of these QDs in the wavelength range between 780 nm and 900 nm is expected to be built on by the continued development of QDs emitting at the telecom bands. Quantum communication experiments utilising QDs have demonstrated their ability to link university campuses and metropolitan areas [30–35]. However, the lack of bright single-photon signals in the telecommunication bands have hindered progress beyond these boundaries to intercity distances. Nevertheless, a recent breakthrough [36] has enabled the emission of bright single photons with high emission rates thanks to Purcell enhancement, from a QD device directly in the telecommunication C-band and therefore expanding the horizons of quantum communication.

Here we report on the first intercity QKD experiments with a deterministic single-photon source. A semiconductor quantum dot embedded in a circular Bragg grating (CBG) efficiently emitting single photons of high purity in the telecommunication C-band is employed in conjunction with polarisation encoding in the standard BB84 protocol [37, 38]. The photons are routed on a 79 km long deployed fibre between

* fei.ding@fkp.uni-hannover.de

the German cities of Hannover and Braunschweig, featuring a loss of (25.49 ± 0.02) dB corresponding to a standard telecom fibre length of 130.32 km. We verify that high-rate secret key transmission and a low quantum bit error ratio (QBER) of $\sim 0.65\%$ are ensured for 35 h. An average secret key bits (SKBs) per pulse of more than 2×10^{-5} in the finite-key regime can be reached over an acquisition time of 30 min. Positive key rates are determined achievable for distances up to 144 km corresponding to 28.11 dB loss in the laboratory, highlighting the competitiveness of semiconductor SPSs for quantum communication applications.

II. OVERVIEW OF THE EXPERIMENT

The intercity experiment is performed in the German federal state of Niedersachsen, in which a deployed fibre of ~ 79 km length connects the Leibniz University of Hannover (LUH) and Physikalisch-Technische Bundesanstalt (PTB) Braunschweig, as depicted in Fig. 1(a). Alice, located at the LUH, statically prepares polarisation-encoded single photons as $\{|H\rangle, |V\rangle, |D\rangle, |A\rangle\}$. Bob, located at the PTB, contains a passive polarisation decoder to measure the polarisation states on two balanced conjugate bases. We denote the rectilinear $\{|H\rangle, |V\rangle\}$ and diagonal $\{|D\rangle, |A\rangle\}$ bases as Z and X bases, respectively.

In the transmitter of Alice, a pulsed laser at a wavelength of 1529.8 nm and with adjustable clock rate (CR) is employed to excite the p-shell of the InAs/InGaAs/GaAs QD mounted into a 4 K helium gas closed-cycle cryostat [Fig. 1(b)]. The QD, embedded in a CBG photonic structure, emits single photons at a wavelength of 1555.9 nm with high brightness. The Purcell effect of the CBG cavity reduces the QD's emission lifetime to (592.5 ± 1.8) ps [39], which theoretically allows for an increase of the excitation CR up to GHz. An average photon number per pulse of $\langle n \rangle = 0.138$ at the first lens [40] is measured with a blinking-corrected $g^{(2)}(0) = (2.43 \pm 0.02)\%$ [39], while the QD is excited at its saturation power. To first study all of the QKD performance for different transmission distances in the lab, encoded single photons are sent through one or multiple standard telecom fibre spools (ITU-T G.652.D) of 40 km length each. The average loss of $l = (0.1956 \pm 0.0026)$ dB/km per spool is calibrated in the laboratory, taking into account the insertion loss (see Supplementary [39]). So as to then realise the intercity QKD experiment over the deployed fibre, a reference signal for local synchronisation is required. Therefore, the single photon signals are transmitted over the intercity link together with attenuated pulses from the excitation laser. On the receiver side, these two signals are de-multiplexed and the single photon states are decoded. Superconducting nanowire single-photon detectors (SNSPDs) are used for detecting the single photons and the reference laser signal, which thereby provides a timing reference to the single photon detection events.

One of the figure of merits used to assess the performance of QKD is the SKBs per pulse. In our work, we study this in

both the asymptotic and finite-key regimes. For the asymptotic case [40–42],

$$S_A = p_{sift} \left\{ \underline{p}_c^{(1)} [1 - h(\bar{e}_1)] - f_{EC} p_c h(e_{tot}) \right\} \quad (1)$$

where $p_{sift} = p_X^2 + (1 - p_X)^2$ is the sifting ratio assuming both QKD bases are used for the key generation; p_X is the bias of the projection basis ($p_X = 0.5$ in our case); $\underline{p}_c^{(1)}$ corresponds to the lower bound of detected events for the single-photon state; $h(\cdot)$ is the binary Shannon entropy function; \bar{e}_1 denotes the upper bound of the QBER for single-photon states and e_{tot} is the total QBER for all photon number states. For convenience, we assume balanced efficiencies of the receiver ports and SNSPD channels for each polarisation basis. f_{EC} describes the error correction inefficiency of the algorithm, p_c indicates the total detection probability of the photon number states [43, 44].

For the case of a finite block size of the keys, we evaluate the SKBs per pulse using the multiplicative Chernoff bound [45, 46],

$$S_F = \frac{\underline{n}_{R,nmp}^{X,Z}}{Rt} \left[1 - h(\bar{\phi}^Z) - \lambda_{EC} - \log_2 \frac{2}{\epsilon_{cor}} - 2 \log_2 \frac{1}{2\epsilon_{PA}} \right]. \quad (2)$$

Here, R is the CR, t is the acquisition time, $\underline{n}_{R,nmp}^{X,Z}$ the lower bound of non-multiphoton emissions in the receiver module for X and Z bases, $\bar{\phi}^Z$ the upper bound of the phase error rate, λ_{EC} the lower bound of information leakage [47] and ϵ_{cor} are the bits used for verification during the error correction process. ϵ_{PA} is the failure probability of privacy amplification. Table I presents both the performance of our QD-based SPS and security parameters of our QKD system, in which we consider ϵ -secret $\epsilon_{sec} = 10^{-10}$ and ϵ -correct $\epsilon_{cor} = 10^{-15}$ for reaching ϵ_{qkd} -secure ($\epsilon_{qkd} \geq \epsilon_{sec} + \epsilon_{cor}$) [48].

Tab. I. QKD system and security parameters.

Description	Parameter	Value
Average photon number per pulse	$\langle n \rangle$	0.138
Clock rate	R	228 MHz
Second-order correlation	$g^{(2)}(0)$	2.43 %
Transmitter efficiency	η_T	0.464
Receiver efficiency	η_R	0.740
System misalignment probability	p_{mis}	2.57×10^{-4}
Detector efficiency	η_D	0.740
Dark count probability	p_{dc}	8.74×10^{-7}
Dead time	τ_{dt}	35.865 ns
Averaged fibre-spool loss	l	0.1956 dB/km
Field-installed fibre loss	L	25.49 dB
Parameter estimation failure probability	ϵ_{PE}	$2 \times 10^{-10}/3$
Error correction failure probability	ϵ_{EC}	$10^{-10}/6$
Privacy amplification failure probability	ϵ_{PA}	$10^{-10}/6$
Error verification failure probability	ϵ_{cor}	10^{-15}
Error correction leakage	f_{EC}	1.16
λ_{EC}	SM [39]	

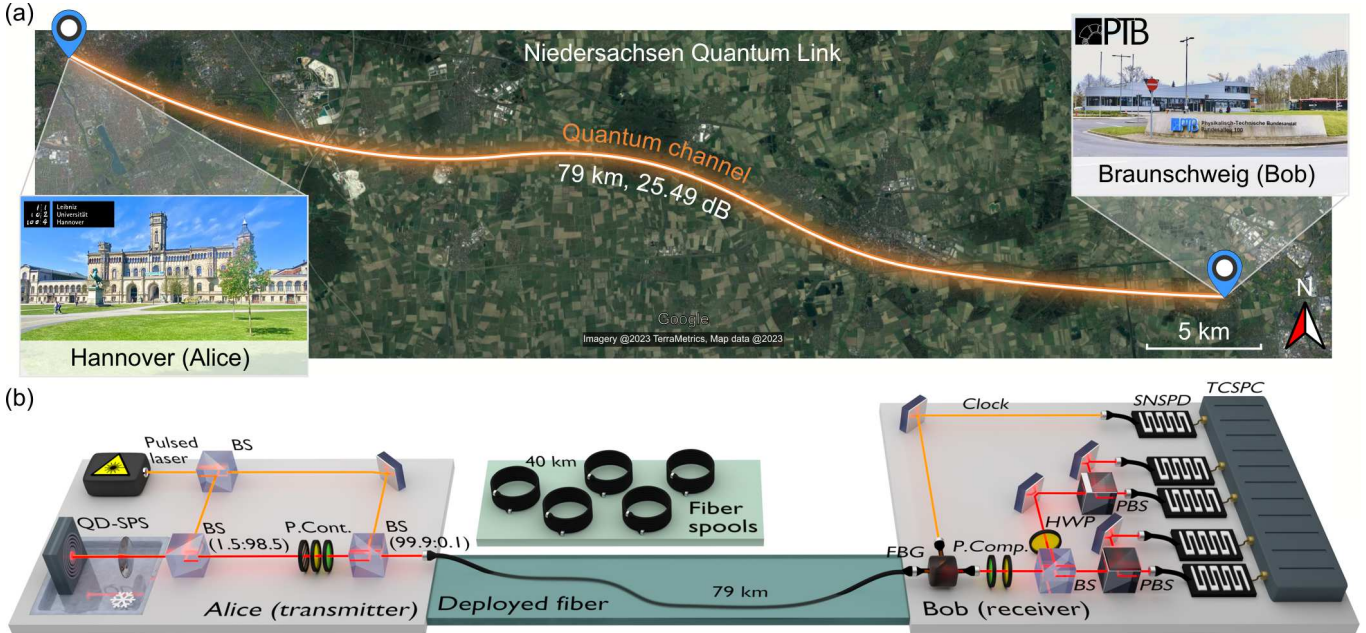


Fig. 1. Overview of the intercity QKD experiments on the ‘Niedersachsen quantum link’ using single photons from a semiconductor quantum dot (QD). (a) Distribution of quantum bits between Hannover (Alice) and Braunschweig (Bob) over 79 km of deployed fibre with a total loss of 25.49 dB. Map data from Google (©2023 Google). (b) Sketch of the experimental setup. The QD-based SPS of the transmitter is mounted in a cryostat and excited by a pulsed laser at different clock rates (CRs) (76 MHz, 228 MHz, 608 MHz, and 1063 MHz). The emitted single photons are collected by an aspherical lens with a numerical aperture of 0.7. State encoding is performed by a polarisation control module (P. Cont.) comprising a polariser, a half-wave plate (HWP) and a quarter-wave plate (QWP). The single-photon and excitation laser signals are then together coupled into either a sequence of fibre spools or the deployed fibre. In the receiver module, a fibre Bragg grating (FBG) demultiplexes the single photon and laser signals by wavelength. An electronically controlled polarisation compensation (P. Comp.) module with QWP and HWP counteracts polarisation fluctuations in the quantum channels by monitoring and minimising the QBER. A non-polarising 50:50 beam splitter (BS) then acts as a random selector of the decoding basis, with rectilinear projection in the transmitted path using a polarisation beam splitter (PBS), and diagonal projection in the reflected path using a HWP at an angle of 22.5° followed by a PBS. The four single-photon signals and the laser signal are detected at superconducting nanowire single-photon detectors (SNSPDs) and the timing events recorded with a time-correlated single-photon counting (TCSPC) unit.

III. SOURCE PERFORMANCE FOR IN-LAB QKD

We now investigate the performance of the semiconductor SPS for the in-lab QKD experiment. In Fig. 2, the SKBs per pulse is shown in dependence of (a) excitation power and (b) temperature. The average photon number per pulse $\langle n \rangle$ and blinking-corrected $g^{(2)}(0)$ are measured and fed into Eq. 1 and 2 [39], assuming a received block size of $n_R^Z = 10^8$ bits for the Z-basis in the finite-key regime. Both the asymptotic and finite SKBs per pulse start to drop above the excitation power of $(2.98 \pm 0.15) \mu\text{W}$ because of a decreasing source brightness due to the damping of Rabi-oscillation under p-shell excitation [49]. In the temperature-dependent measurement, we observe that the values degrade by $\sim 50\%$ upon tuning the temperature from 4 K to 34 K mainly because of a reduced brightness and single photon purity [36]. Nevertheless, the well preserved overall performance would allow employing compact cryogenic cooling systems, indicating feasibility for commercial plug-and-play QKD systems.

To assess the performance of semiconductor SPS based QKD for long-distance transmission, we study the SKBs per pulse over varying transmission loss in the laboratory, as

shown in Fig. 2(c). The QD is pumped with a CR of 228 MHz and the emitted single photon signal is coupled into the fibre spools mentioned above. To emulate distances of 20 km and 60 km, we added a variable fibre optical attenuator with a fixed loss of (4.0 ± 0.4) dB. To obtain the data points, the truth table and second-order auto-correlation measurements are recorded based on the statically encoded polarisation qubits at each transmission loss, in order to extract the average photon number per pulse ($\langle n \rangle$), quantum bit error ratio (QBER) (e_{tot}), and single photon purity [39]. The solid lines in Fig. 2(c) illustrate the simulation of QBER and SKBs per pulse by employing the values of parameters measured from the QD (Tab. I). With an increased block size n_R^Z in the finite-key regime, the simulated maximum tolerable loss (MTL) approaches the one for the asymptotic regime at 28.11 dB, corresponding to a transmission distance of 141.05 km in a standard telecommunication fibre. In this experiment, the MTL for both the asymptotic and finite-key block cases are limited by the blinking-corrected $g^{(2)}(0)$, since the multi-photon emission probability is detrimental for generating high SKRs with single-photon states in the high-loss regime. The SKR and MTL can be improved by employing adequate pre-attenuation [46] and employing time

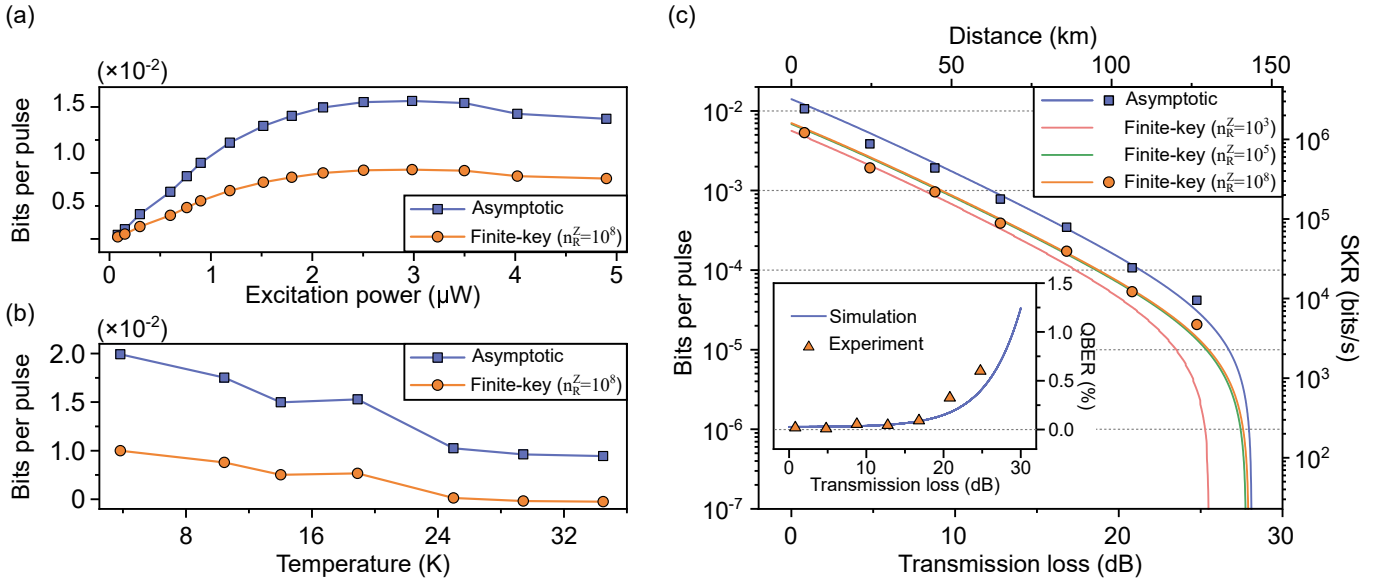


Fig. 2. In-lab characterisation of the QD based single-photon source and the experimental setup. Secret key per clock pulse as a function of (a) excitation laser power and (b) of temperature in the asymptotic and finite-key regime. (c) Secret key bits (SKBs) per pulse as a function of the transmission loss. The maximum tolerable losses (MTLs) for the asymptotic case and finite-key block cases with different block sizes of $n_R^Z = 10^3, 10^5, 10^8$ are extracted to be 28.11, 25.51, 27.78 and 27.95 dB, respectively. The inset shows the measured and simulated quantum bit error ratio (QBER) as a function of transmission loss with the dashed grey line indicating the QBER at zero.

gating on the histograms of second-order correlation and truth table during post-processing [44, 50].

One outstanding feature of SPS is the on-demand photon emission, allowing ultra-high photon count rates with GHz CRs [51, 52]. To explore the CR-dependent SKR capabilities of our system, we perform the truth table measurements using 80 km of fibre spool and different excitation laser CRs. The QBER, Asymptotic-SKR (A-SKR), and Finite-SKR (F-SKR) are extracted from the truth tables as shown in Tab. II. The QBER decreases with increasing CR due to the lower dark count contributions resulting from smaller integration windows. Although the SKR is limited by the QD lifetime and detector dead times, the achievable high SKRs of $> 100\text{ kbit/s}$ would enable QKD secured live video conferences encrypted with an one-time-pad (OTP) encryption [53–55].

Tab. II. Averaged QBER, A-SKR and F-SKR ($n_R^Z = 10^8$) measured under different CRs for the fibre spool distance of 80 km

CR (MHz)	QBER (%)	A-SKR (kbit/s)	F-SKR (kbit/s)
76	0.344	28.12	14.19
228	0.099	67.97	33.88
608	0.089	151.57	75.93
1063	0.064	216.74	108.36

IV. INTERCITY QKD OVER THE DEPLOYED FIBRE

Now, the intercity QKD experiments are performed by sending telecom C-band single photons emitted by the semiconductor QD SPS from Hannover to Braunschweig via the

‘Niedersachsen Quantum Link’. In the optics lab in Braunschweig (Bob), time traces of the single photon emission under different CRs are obtained by correlating the reference laser and single photon signals [Fig. 3(a)]. For CRs ranging from 76 MHz up to 1.06 GHz the single photon pulse trains are clearly identified. Still, at 608 MHz and above the peaks start to overlap, implying a saturation in the achievable photon counts for high CRs. Fig. 3(b) represents a continuous second-order auto-correlation measurement of up to 12 h at the deployed fibre end in Braunschweig. The blinking-corrected $g^{(2)}(0)$ plotted over the measurement time reveals high and stable single-photon purity which is important for long-term communication applications. The single-photon purity is preserved at $> 85\%$ for the first three CRs and reduces to $\sim 81.5\%$ for 1063 MHz due to coincidence events involving photons from adjacent pulse trains, as visible from the right inset graph. It has to be noted that no temporal filtering has been applied here, which could be used to increase the single-photon purity at higher CRs at the expense of the number of coincidences. The higher blinking-corrected $g^{(2)}(0)$ under 76 MHz in comparison to 228 MHz is due to the contribution of dark counts due to a wider temporal coincidence window (the inverse CR).

To evaluate the performance of real-world QKD over the fibre link, the truth table is measured by accumulating the coincidence histograms between the reference laser and QD signals from the receiver ports, while four polarisation states are statically encoded by the transmitter. An automatic polarisation compensation algorithm at the receiver is developed by minimising the locally measured QBER, in order to counteract polarisation fluctuations of the fibre link (see Supplementary [39]). Fig. 3(c) illustrates the normalised truth ta-

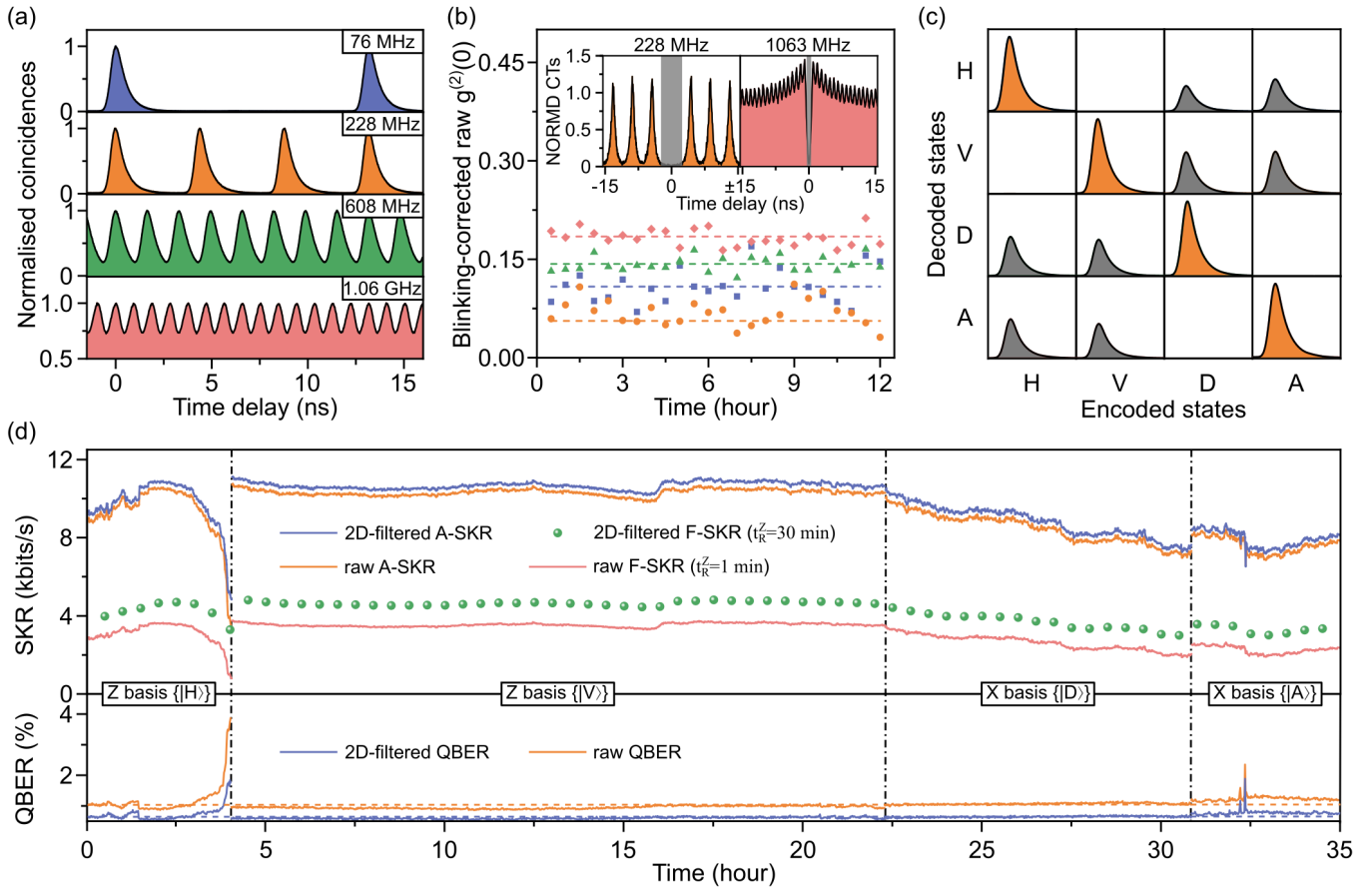


Fig. 3. Intercity quantum key distribution with telecom C-band single photons from a semiconductor source, transmitted over the deployed fibre. (a) Time-resolved QD emission for different CRs. (b) Blinking-corrected, second-order auto-correlation at zero time delay $g^{(2)}(0)$ as a function of measurement time recorded in Braunschweig for the CRs $\blacksquare 76\text{ MHz}$, $\bullet 228\text{ MHz}$, $\blacktriangle 608\text{ MHz}$, and $\blacklozenge 1.06\text{ GHz}$. Each data point represents 0.5 h of measurement time, and no time gating was applied. The dashed lines show the average $g^{(2)}(0)$ over the whole measurement with values of 0.108 ± 0.005 , 0.056 ± 0.002 , 0.143 ± 0.002 , and 0.185 ± 0.002 . Insets: Normalised (NORMD) second-order correlation histograms for the CRs of 228 MHz and 1064 MHz. (c) Truth table of the polarisation encoded BB84 protocol. The correlation histograms in each column are normalised by the decoded coincidences resulting from the encoded states (diagonal histograms in the table). (d) A-SKR, F-SKR, and QBER over time for different encoding bases $\{X, Z\}$ at a fixed CR of 228 MHz. Each data point in the solid lines represents the average of 1 min. Average asymptotic and finite SKBs per pulse over the 35 h key transmission time with and without the 2-D temporal filter are evaluated to be 4.80×10^{-5} , 4.64×10^{-5} , 2.35×10^{-5} , 1.87×10^{-5} . The average QBER (dashed line) decreases from 1.04 % to 0.65 %.

ble, obtained with a CR of 228 MHz and a measurement time of more than 6 h for each encoded state. The diagonal histograms in the table correspond to the sifted keys that are usable for error correction and privacy amplification, and the grey histograms illustrate the discarded keys by basis sifting. A fidelity of 99.6 % is extracted from the projection on the ideal truth table with flawless key decryption. By now measuring the time-dependent truth table, eventually the A-SKR, F-SKR, and QBER time traces are obtained and displayed in Fig. 3(d). In addition to extracting the raw time tags, temporal filtering with a 2D-filter is applied by monitoring the $g^{(2)}$ and truth table histograms in order to maximise the SKRs and minimise the QBERs [39, 50]. The fluctuation of the SKR and QBER while the $|H\rangle$ state is projected onto Z basis, results from the sensitive fibre coupling of $|H\rangle$ signals on the receiver module. Nevertheless, the averaged QBER of 0.65 %

over such a transmission loss is the lowest value achieved so far in QKDs with SPSs. This leads to efficient extraction of secret keys from the X basis, according to the keys sifted by the Z basis for phase error rate estimation. The average A-SKR and F-SKR are then obtained to be (10.93 ± 1.19) kbit/s and (5.35 ± 0.58) kbit/s, respectively. Such SKRs allow for, e.g., live encryption of speech between the two cities via the shared keys [56].

V. COMPARISON WITH STATE-OF-THE-ART

Here we present a comparative analysis involving other SPS-based QKD experiments and the high-rate decoy-state BB84 protocol in the telecom C-band as depicted in Fig. 4. Recent QKD implementations have reported two noteworthy

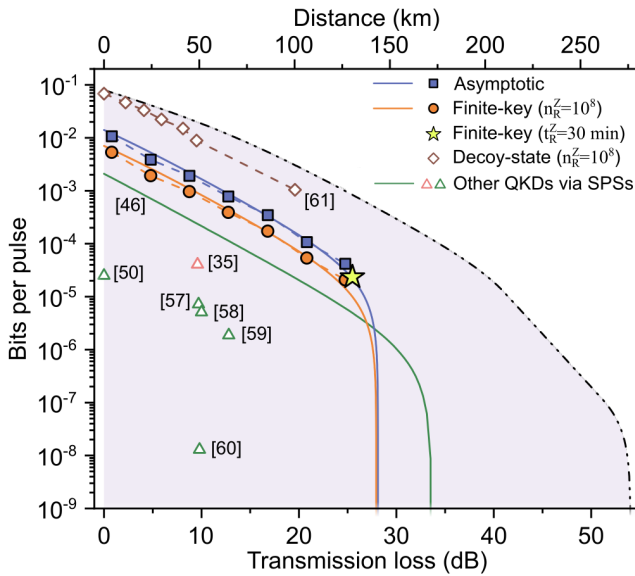


Fig. 4. Comparison of the SKBs per pulse with other QKD experiments. The in-lab SKBs per pulse (■, ●) and the field-based SKBs per pulse in the finite-key regime (★) surpass previous realisations based on single-photon sources with photons in the telecom C-band and approach state-of-the-art decoy state QKD. The triangles (△, ▲) show the QKDs with SPSs based via deployed fibre and fibre spools, respectively. The solid lines represent simulated SKBs per pulse using the experimental parameters. The dashed, black line represents the SKBs per pulse that is achievable with experimentally feasible source optimisations. Corresponding distance is calculated for 0.1956 dB/km standard telecommunication fibre.

approaches, both utilizing SPSs. The first involves QDs in photonic crystal waveguides [35], while the second employs a QD contained in an oxide-apertured micropillar [46]. Both SPS were not directly emitting into the telecom C-band, and therefore frequency conversion techniques were employed, introducing additional losses. In contrast, our implementation features a highly efficient source emitting at the telecom C-band, and both simulation and experimental data reveal a substantial increase in the SKBs per pulse for data transmission.

Furthermore, we illustrate the asymptotic SKBs per pulse from other QKDs based on telecom single photon emitters [50, 57–60]. Notably, the achieved finite SKBs per pulse over the intercity fibre testbed, denoted by a star, also represents the highest SKR achieved to date in SPS-based QKD under 228 MHz CR. In addition, our results approach the current record of finite SKBs per pulse achieved by decoy-state BB84 with weak coherent pulses in laboratory settings [61].

The demonstrated QKD performance can be further enhanced through optimisations of source quality, detection systems, and protocols. The shaded purple region, delineated by a black dash line, represents an emulation of the achievable asymptotic SKBs per pulse by considering experimentally accessible parameters, such as an improved source efficiency [62], single-photon purity [63], and system dark counts [16]. Regarding the protocol, optimal pre-attenuation of single-photon counts [46] and an asymmetric projection basis choice

[64] for each individual transmission loss result in higher SKR and MTL without compromising security. By incorporating these feasible primary parameters, we anticipate achieving a MTL of 54.1 dB, corresponding to a distance of 276.58 km in the asymptotic regime. Furthermore, a SKR approaching 1 MHz under a transmission loss of approximately 25 dB is attainable assuming a CR of 1 GHz, a configuration well-suited for distributed secure storage [65]. For a more comprehensive comparison of our findings with other QKD protocols, refer to the Supplementary [39].

VI. CONCLUSION

In conclusion, the first intercity QKD experiments using a deterministic telecom SPS has been demonstrated. This advancement was made possible by harnessing single-photon emissions from a semiconductor QD embedded in a CBG structure, emitting within the telecom C-band and excitation rates up to the GHz range. SKRs have been investigated for different temperatures, excitation powers, and transmission losses under both asymptotic and finite-key scenarios. The measurements and simulations indicate an asymptotic MTL of 28.11 dB, corresponding to 143.71 km channel length in repeaterless quantum communication with standard fibre-optic networks. The experiment spanned a deployed optical fibre link of approximately 79 km and a total loss of 25.49 dB, over which high-rate secret key transmission over an extended period of 35 h is obtained. The averaged QBER is impressively low at around 0.65 %, highlighting the robustness and reliability of the system. Comparative analysis with existing QKD systems involving SPS reveals that the SKR achieved in this work goes beyond all current SPS based implementations. Even without further optimisation of the source and setup performance it approaches the levels attained by established decoy state QKD protocols based on weak coherent pulses. This outcome underscores the viability of seamlessly integrating semiconductor single-photon sources into realistic, large-scale and high-capacity quantum communication networks. Moreover, semiconductor QDs, acting as high-speed and deterministic single-photon emitters, hold promising implications for MDI-QKD and may serve as enablers for quantum repeater based star-like networks.

AUTHOR CONTRIBUTION

J. Yang and R. Joos implemented the optical characterisation of the sample. J. Yang, Z. Jiang, F. Benthin and J. Hanel, A. Hreibi and M. Zopf carried out the QKD experiment. S. Bauer, S. Kolatschek, and M. Jetter designed and fabricated the sample. T. Fandrich, J. Hanel, J. Yang, F. Benthin and Z. Jiang performed the data analysis and the interpretation of the results. J. Yang wrote the manuscript with the help from M. Zopf, F. Ding, E. P. Rugeramigabo, S.L. Portalupi, P. Michler, and the other co-authors. F. Ding, P. Michler, and S. Kück conceived and supervised the project.

ACKNOWLEDGMENTS

We thank J. Wang, C. Nawrath, M. Auer and T. van Leent for fruitful discussions, and R. Guan for helping with the optical setups. We thank J. Kronjäger, A.K. Kniggendorf and A. Kuhl for efficiently organising the deployed fiber infrastructure. We would also like to thank PriTel Inc. for their continued and timely support.

FUNDING

The authors gratefully acknowledge the funding by the German Federal Ministry of Education and Research (BMBF)

within the project QR.X (16KISQ013 and 16KISQ015), SQuaD (16KISQ117), InterSync (GZ: INST 187/880-1 AOBJ: 683478) and SemIQON (13N16291), the European Research Council (QD-NOMS GA715770, MiNet GA101043851), European Union's Horizon 2020 research and innovation program under Grant Agreement No. 899814 (Qurope), EMPIR programme co-financed by the Participating States and from the European Union's Horizon 2020 research and innovation programme (20FUN05 SEQUME), the Deutsche Forschungsgemeinschaft (DFG, German Research Foundation) under Germany's Excellence Strategy (EXC-2123) QuantumFrontiers (390837967), and Flexible Funds programme by Leibniz University Hannover (51410122).

[1] S. Wehner, D. Elkouss, and R. Hanson, *Science* **362**, 6412 (2018).

[2] L. Gyongyosi and S. Imre, *Commun. ACM* **65**, 52 (2022).

[3] C. H. Bennett, G. Brassard, C. Crépeau, R. Jozsa, A. Peres, and W. K. Wootters, *Phys. Rev. Lett.* **70**, 1895 (1993).

[4] D. Boschi, S. Branca, F. D. Martini, L. Hardy, and S. Popescu, *Phys. Rev. Lett.* **80**, 1121 (1998).

[5] D. Bouwmeester, J.-W. Pan, K. Mattle, M. Eibl, H. Weinfurter, and A. Zeilinger, *Nature* **390**, 575 (1997).

[6] H. Soeparno and A. S. Perbangsa, *Procedia Comput. Sci.* **179**, 944 (2021).

[7] N. Taleb and E. A. Mohamed, *Academic Journal of interdisciplinary studies* **9** (2020).

[8] T. Qian, J. Bringewatt, I. Boettcher, P. Bienias, and A. V. Gorshkov, *Phys. Rev. A* **103**, 1030601 (2021).

[9] W. Ge, K. Jacobs, Z. Eldredge, A. V. Gorshkov, and M. Foss-Feig, *Phys. Rev. Lett.* **121**, 043604 (2018).

[10] S. Aaronson and L. Chen, in *32nd Computational Complexity Conference (CCC 2017)*, Leibniz International Proceedings in Informatics (LIPIcs), Vol. 79, edited by R. O'Donnell (Schloss Dagstuhl—Leibniz-Zentrum fuer Informatik, Dagstuhl, Germany, 2017) pp. 22:1–22:67.

[11] J. Preskill, *Quantum* **2**, 79 (2018).

[12] H.-S. Zhong, H. Wang, Y.-H. Deng, M.-C. Chen, L.-C. Peng, Y.-H. Luo, J. Qin, D. Wu, X. Ding, Y. Hu, P. Hu, X.-Y. Yang, W.-J. Zhang, H. Li, Y. Li, X. Jiang, L. Gan, G. Yang, L. You, Z. Wang, L. Li, N.-L. Liu, C.-Y. Lu, and J.-W. Pan, *Science* **370**, 1460 (2020).

[13] H.-K. Lo, M. Curty, and K. Tamaki, *Nat. Photonics* **8**, 595 (2014).

[14] R. L. Rivest, A. Shamir, and L. Adleman, *Commun. ACM* **21**, 120 (1978).

[15] J.-P. Chen, C. Zhang, Y. Liu, C. Jiang, W.-J. Zhang, Z.-Y. Han, S.-Z. Ma, X.-L. Hu, Y.-H. Li, H. Liu, F. Zhou, H.-F. Jiang, T.-Y. Chen, H. Li, L.-X. You, Z. Wang, X.-B. Wang, Q. Zhang, and J.-W. Pan, *Nat. Photonics* **15**, 570 (2021).

[16] Y. Liu, W.-J. Zhang, C. Jiang, J.-P. Chen, C. Zhang, W.-X. Pan, D. Ma, H. Dong, J.-M. Xiong, C.-J. Zhang, H. Li, R.-C. Wang, J. Wu, T.-Y. Chen, L. You, X.-B. Wang, Q. Zhang, and J.-W. Pan, *Phys. Rev. Lett.* **130**, 210801 (2023).

[17] R. Bedington, J. M. Arrazola, and A. Ling, *npj Quantum Inf.* **3**, 30 (2017).

[18] C.-Y. Lu, Y. Cao, C.-Z. Peng, and J.-W. Pan, *Rev. Mod. Phys.* **94**, 035001 (2022).

[19] V. Scarani, H. Bechmann-Pasquinucci, N. J. Cerf, M. Dušek, N. Lütkenhaus, and M. Peev, *Rev. Mod. Phys.* **81**, 1301 (2009).

[20] H.-J. Briegel, W. Dür, J. I. Cirac, and P. Zoller, *Phys. Rev. Lett.* **81**, 5932 (1998).

[21] F. Xu, X. Ma, Q. Zhang, H.-K. Lo, and J.-W. Pan, *Rev. Mod. Phys.* **92**, 025002 (2020).

[22] J. Schneeloch, S. H. Knarr, D. F. Bogorin, M. L. Levangie, C. C. Tison, R. Frank, G. A. Howland, M. L. Fanto, and P. M. Alsing, *J. Opt.* **21**, 043501 (2019).

[23] W.-Y. Hwang, *Phys. Rev. Lett.* **91**, 057901 (2003).

[24] C.-Y. Lu and J.-W. Pan, *Nat. Nanotechnol.* **16**, 1294 (2021).

[25] D. A. Vajner, L. Rickert, T. Gao, K. Kaymazlar, and T. Heindel, *Adv. Quantum Technol.* **5**, 2100116 (2022).

[26] C. Couteau, S. Barz, T. Durt, T. Gerrits, J. Huwer, R. Prevedel, J. Rarity, A. Shields, and G. Weihs, *Nature Reviews Physics* **5**, 326 (2023).

[27] Y.-H. Zhou, Z.-W. Yu, A. Li, X.-L. Hu, C. Jiang, and X.-B. Wang, *Sci. Rep.* **8**, 4115 (2018).

[28] L. Zaporski, N. Shofer, J. H. Bodey, S. Manna, G. Gillard, M. H. Appel, C. Schimpf, S. F. C. da Silva, J. Jarman, G. Delamare, G. Park, U. Haeusler, E. A. Chekhovich, A. Rastelli, D. A. Gangloff, M. Atatüre, and C. L. Gall, *Nat. Nanotechnol.* **18**, 257 (2023).

[29] I. Schwartz, D. Cogan, E. R. Schmidgall, Y. Don, L. Gantz, O. Kenneth, N. H. Lindner, and D. Gershoni, *Science* **354**, 434 (2016).

[30] R. Alléaume, F. Treussart, G. Messin, Y. Dumeige, J.-F. Roch, A. Beveratos, R. Bouri-Tualle, J.-P. Poizat, and P. Grangier, *New J. Phys.* **6**, 92 (2004).

[31] M. Rau, T. Heindel, S. Unsleber, T. Braun, J. Fischer, S. Frick, S. Nauerth, C. Schneider, G. Vest, S. Reitzenstein, M. Kamp, A. Forchel, S. Höfling, and H. Weinfurter, *New J. Phys.* **16**, 043003 (2014).

[32] Z.-H. Xiang, J. Huwer, R. M. Stevenson, J. Skiba-Szymanska, M. B. Ward, I. Farrer, D. A. Ritchie, and A. J. Shields, *Sci. Rep.* **9**, 10,1038/s41598-019-40912-z (2019).

[33] F. B. Basset, M. Valeri, E. Roccia, V. Muredda, D. Poderini, J. Neuwirth, N. Spagnolo, M. B. Rota, G. Carvacho, F. Sciarino, and R. Trotta, *Sci. Adv.* **7**, eabe6379 (2021).

[34] C. Schimpf, M. Reindl, D. Huber, B. Lehner, S. F. C. D. Silva, S. Manna, M. Vyvlecka, P. Walther, and A. Rastelli, *Sci. Adv.* **7**, eabe8905 (2021).

[35] M. Zahidy, M. T. Mikkelsen, R. Müller, B. Da Lio, M. Krehbiel, Y. Wang, N. Bart, A. D. Wieck, A. Ludwig, M. Galili, S. Forchhammer, P. Lodahl, L. K. Oxenløwe, D. Bacco, and L. Midolo, *Quantum key distribution using deterministic single-photon sources over* (2023), arXiv:2301.09399 [quant-ph].

[36] C. Nawrath, R. Joos, S. Kolatschek, S. Bauer, P. Pruy, F. Hornung, J. Fischer, J. Huang, P. Vijayan, R. Sittig, M. Jetter, S. L. Portalupi, and P. Michler, *High emission rate from a purcell-enhanced, triggered source of pure single photons* (2022), arXiv:2207.12898 [quant-ph].

[37] C. H. Bennett and G. Brassard, in *Proceedings of IEEE International Conference on Computers, Systems, and Applications* (Zürich, 1984) p. 175.

[38] C. H. Bennett and G. Brassard, *Theoret. Comput. Sci.* **560**, 7 (2014).

[39] See supplemental material at [url will be inserted by the production group] for more experimental details and data analysis (2023).

[40] E. Waks, C. Santori, and Y. Yamamoto, *Phys. Rev. A* **66**, 042315 (2002).

[41] D. Gottesman, H.-K. Lo, N. Lütkenhaus, and J. Preskill, *Proc. Natl. Acad. Sci. U.S.A.* **101**, 325 (2004).

[42] R. Y. Q. Cai and V. Scarani, *New J. Phys.* **11**, 045024 (2009).

[43] M. Bozzio, M. Vyvlecka, M. Cosacchi, C. Nawrath, T. Seidelmann, J. C. Loredo, S. L. Portalupi, V. M. Axt, P. Michler, and P. Walther, *npj Quantum Inf.* **8**, 104 (2022).

[44] M. Vyvlecka, L. Jehle, C. Nawrath, F. Giorgino, M. Bozzio, R. Sittig, M. Jetter, S. L. Portalupi, P. Michler, and P. Walther, *Robust excitation of c-band quantum dots for enhanced quantum communication* (2023), arXiv:2305.13273 [quant-ph].

[45] H.-L. Yin, M.-G. Zhou, J. Gu, Y.-M. Xie, Y.-S. Lu, and Z.-B. Chen, *Sci. Rep.* **10**, 14312 (2020).

[46] C. L. Morrison, R. G. Pousa, F. Graffitti, Z. X. Koong, P. Barrow, N. G. Stoltz, D. Bouwmeester, J. Jeffers, D. K. L. Oi, B. D. Gerardot, and A. Fedrizzi, *Nat Commun* **14**, 3573 (2023).

[47] M. Tomamichel, J. Martínez-Mateo, C. Pacher, and D. Elkouss, *Quantum Inf. Process.* **16**, 280 (2017).

[48] D. Bunandar, L. C. G. Govia, H. Krovi, and D. Englund, *npj Quantum Inf.* **6**, 104 (2020).

[49] P. Ester, L. Lackmann, M. Hübner, S. M. de Vasconcellos, A. Zrenner, and M. Bichler, *Phys. E: Low-Dimens. Syst. Nanostructures* **40**, 2004 (2008).

[50] T. Gao, L. Rickert, F. Urban, J. Große, N. Srocka, S. Rodt, A. Musiał, K. Żolnacz, P. Mergo, K. Dybka, W. Urbańczyk, G. Sek, S. Burger, S. Reitzenstein, and T. Heindel, *Appl. Phys. Rev.* **9**, 011412 (2021).

[51] A. Schleehahn, A. Thoma, P. Munnely, M. Kamp, S. Höfling, T. Heindel, C. Schneider, and S. Reitzenstein, *APL Photonics* **1**, 10.1063/1.4939831 (2016).

[52] G. Shooter, Z.-H. Xiang, J. R. A. Müller, J. Skiba-Szymanska, J. Huwer, J. Griffiths, T. Mitchell, M. Anderson, T. Müller, A. B. Krysa, R. M. Stevenson, J. Heffernan, D. A. Ritchie, and A. J. Shields, *Opt. Express* **28**, 36838 (2020).

[53] M. Sasaki, M. Fujiwara, H. Ishizuka, W. Klaus, K. Wakui, M. Takeoka, S. M. Shields, T. Yamashita, Z. Wang, A. Tanaka, K. Yoshino, Y. Nambu, S. Takahashi, A. Tajima, A. Tomita, T. Domeki, T. Hasegawa, Y. Sakai, H. Kobayashi, T. Asai, K. Shimizu, T. Tokura, T. Tsurumaru, M. Matsui, T. Honjo, K. Tamaki, H. Takesue, Y. Tokura, J. F. Dynes, A. R. Dixon, A. Poppe, A. Allacher, O. Maurhart, T. Längler, M. Peev, and A. Zeilinger, *Opt. Express* **19**, 10387 (2011).

[54] S.-K. Liao, W.-Q. Cai, J. Handsteiner, B. Liu, J. Yin, L. Zhang, D. Rauch, M. Fink, J.-G. Ren, W.-Y. Liu, Y. Li, Q. Shen, Y. Cao, F.-Z. Li, J.-F. Wang, Y.-M. Huang, L. Deng, T. Xi, L. Ma, T. Hu, L. Li, N.-L. Liu, F. Koidl, P. Wang, Y.-A. Chen, X.-B. Wang, M. Steindorfer, G. Kirchner, C.-Y. Lu, R. Shu, R. Ursin, T. Scheidl, C.-Z. Peng, J.-Y. Wang, A. Zeilinger, and J.-W. Pan, *Phys. Rev. Lett.* **120**, 030501 (2018).

[55] D. Zhu, J. Zheng, H. Zhou, J. Wu, N. Li, and L. Song, *Mathematics* **10**, 3037 (2022).

[56] A. McCree and T. Barnwell, *IEEE Trans. Speech Audio Processing* **3**, 242 (1995).

[57] K. Takemoto, Y. Nambu, T. Miyazawa, Y. Sakuma, T. Yamamoto, S. Yorozu, and Y. Arakawa, *Sci. Rep.* **5**, 14383 (2015).

[58] K. Takemoto, Y. Nambu, T. Miyazawa, K. Wakui, S. Hirose, T. Usuki, M. Takatsu, N. Yokoyama, K. Yoshino, M. Takeoka, S. Yorozu, Y. Sakuma, and Y. Arakawa, *Appl. Phys. Express* **3**, 092802 (2010).

[59] P. M. Intallura, M. B. Ward, O. Z. Karimov, Z. L. Yuan, P. See, A. J. Shields, P. Atkinson, and D. A. Ritchie, *Appl. Phys. Lett.* **91**, 161103 (2007).

[60] A. Soujaeff, T. Nishioka, T. Hasegawa, S. Takeuchi, T. Tsurumaru, K. Sasaki, and M. Matsui, *Opt. Express* **15**, 726 (2007).

[61] W. Li, L. Zhang, H. Tan, Y. Lu, S.-K. Liao, J. Huang, H. Li, Z. Wang, H.-K. Mao, B. Yan, Q. Li, Y. Liu, Q. Zhang, C.-Z. Peng, L. You, F. Xu, and J.-W. Pan, *Nat. Photonics* **17**, 416 (2023).

[62] N. Tomm, A. Javadi, N. O. Antoniadis, D. Najar, M. C. Löbl, A. R. Korsch, R. Schott, S. R. Valentini, A. D. Wieck, A. Ludwig, and R. J. Warburton, *Nat. Nanotechnol.* **16**, 399 (2021).

[63] L. Schweickert, K. D. Jöns, K. D. Zeuner, S. F. C. da Silva, H. Huang, T. Lettner, M. Reindl, J. Zichi, R. Trotta, A. Rastelli, and V. Zwiller, *Appl. Phys. Lett.* **112**, 10.1063/1.5020038 (2018).

[64] H.-K. Lo, H. Chau, and M. Ardehali, *J. Cryptology* **18**, 133 (2004).

[65] M. Sasaki, *Quantum Sci. Technol.* **2**, 020501 (2017).